

## Supporting Information

for *Adv. Opt. Mater.*, DOI: 10.1002/adom.((please add manuscript number))

### Metamaterial analogue of Ising model

*Longqing Cong, Vassili Savinov, Yogesh Kumar Srivastava, Song Han, and Ranjan Singh\**

#### Supplementary Note 1: Multipole decomposition

The relative radiating power of the multipole moments is calculated with the general expression:

$$I = \frac{2\omega^4}{3c^3} |P|^2 + \frac{2\omega^4}{3c^3} |M|^2 + \frac{4\omega^5}{3c^4} (P \cdot T) + \frac{2\omega^6}{3c^5} |T|^2 + \frac{\omega^6}{5c^5} Q_{\alpha\beta}^{(e)} Q_{\alpha\beta}^{(e)} + \frac{\omega^6}{20c^5} Q_{\alpha\beta}^{(m)} Q_{\alpha\beta}^{(m)} + \frac{2\omega^6}{15c^5} (M \cdot \langle R_M^2 \rangle) + o\left(\frac{1}{c^5}\right) \quad \text{S1.1}$$

that is derived to the 5<sup>th</sup> order of  $(1/c)$  in harmonic excitation  $\sim \exp(i\omega t)$ . The terms in the expression are scattered power by: electric dipole, magnetic dipole, the interference between the electric and toroidal dipoles, toroidal dipole, electric quadrupole, magnetic quadrupole, and the correction due to the interference between the magnetic dipole and the first-order mean-square radius of the magnetic dipole distribution.

The multipole moments are calculated from the current density distributions given by Radescu and Vaman. By integrating over the charge density  $\rho(\mathbf{r})$  or current density  $J(\mathbf{r})$  distribution with the unit cell, we are able to compute the multipoles in Cartesian coordinate as:

$$P_\alpha = \int d^3r \rho r_\alpha = \frac{1}{i\omega} \int d^3r J_\alpha, \quad \text{S1.2}$$

$$M_\alpha = \frac{1}{2c} \int d^3r (\mathbf{r} \times \mathbf{J})_\alpha, \quad \text{S1.3}$$

$$T_\alpha = \frac{1}{10c} \int d^3r [(\mathbf{r} \cdot \mathbf{J}) r_\alpha - 2r^2 J_\alpha], \quad \text{S1.4}$$

$$\begin{aligned} Q_{\alpha,\beta}^{(e)} &= \frac{1}{2} \int d^3r \rho [r_\alpha r_\beta - \frac{1}{3} \delta_{\alpha,\beta} r^2] \\ &= \frac{1}{i2\omega} \int d^3r [r_\alpha J_\beta + r_\beta J_\alpha - \frac{2}{3} \delta_{\alpha,\beta} (\mathbf{r} \cdot \mathbf{J})], \end{aligned} \quad \text{S1.5}$$

$$Q_{\alpha,\beta}^{(m)} = \frac{1}{3c} \int d^3r [(\mathbf{r} \times \mathbf{J})_\alpha r_\beta + (\mathbf{r} \times \mathbf{J})_\beta r_\alpha], \quad \text{S1.6}$$

$$Q_{\alpha,\beta}^{(T)} = \frac{1}{28c} \int d^3r [4r_\alpha r_\beta (\mathbf{r} \cdot \mathbf{J}) - 5r^2 (r_\alpha J_\beta + r_\beta J_\alpha) + 2r^2 (\mathbf{r} \cdot \mathbf{J}) \delta_{\alpha,\beta}], \quad \text{S1.7}$$

$$\langle R_M^2 \rangle = \frac{1}{2c} \int d^3r (\mathbf{r} \times \mathbf{J}) r^2 \quad \text{S1.8}$$

$$\begin{aligned} O_{\alpha,\beta,\gamma}^{(e)} &= \frac{1}{6} \int d^3r \rho r_\alpha \left( \frac{r_\beta r_\gamma}{3} - \frac{1}{5} r^2 \delta_{\beta,\gamma} \right) + \{\alpha \leftrightarrow \beta, \gamma\} + \{\alpha \leftrightarrow \gamma, \beta\} \\ &= \frac{1}{i6\omega} \int d^3r \left[ J_\alpha \left( \frac{r_\beta r_\gamma}{3} - \frac{1}{5} r^2 \delta_{\beta,\gamma} \right) + r_\alpha \left( \frac{J_\beta r_\gamma}{3} + \frac{r_\beta J_\gamma}{3} - \frac{2}{5} (\mathbf{r} \cdot \mathbf{J}) \delta_{\beta,\gamma} \right) \right] \\ &\quad + \{\alpha \leftrightarrow \beta, \gamma\} + \{\alpha \leftrightarrow \gamma, \beta\}, \end{aligned}$$

$$O_{\alpha,\beta,\gamma}^{(m)} = \frac{15}{2c} \int d^3r \left( r_\alpha r_\beta - \frac{r^2}{5} \delta_{\alpha,\beta} \right) \cdot [\mathbf{r} \times \mathbf{J}]_\gamma + \{\alpha \leftrightarrow \beta, \gamma\} + \{\alpha \leftrightarrow \gamma, \beta\}. \quad \text{S1.9}$$

Here, we use  $\int d^3r [\mathbf{r} \times \mathbf{J}]_\alpha r_\beta + \{\alpha \leftrightarrow \beta\}$  to represent  $\int d^3r [\mathbf{r} \times \mathbf{J}]_\alpha r_\beta + \int d^3r [\mathbf{r} \times \mathbf{J}]_\beta r_\alpha$  for

simplicity and clarity by exchanging the subscripts of the two terms and  $\alpha, \beta, \gamma = x, y, z$ .

## Supplementary Note 2: Interaction energy analysis

We start from the basic Lagrangian in Eq. 1. The interaction term, amongst other things

describes the interactions between the TASRs in the metamaterial. Such interaction will be linear in excitation amplitude of each meta-molecule, and since we choose to describe the excitation of the whole metamaterial with a single dynamic variable  $X$ , the interaction term of the Lagrangian will be quadratic in excitation amplitude. The most general form is

$$\int_{inter-resonator} d^3r(\rho\phi - \mathbf{A}\cdot\mathbf{J}) = \frac{\alpha X^2}{2} + \frac{\beta X\dot{X}}{\omega_0} + \frac{\dot{X}^2}{2\omega_0^2}. \quad \text{It is then easy to show that}$$

Lagrangian in Eq. 1 with such interactions will lead to equation of motion:

$$\ddot{X} = -\Omega^2 X, \quad \Omega = \sqrt{\frac{\omega_0^2 + \alpha}{1 - \frac{\gamma}{\omega_0^2}}} \approx \omega_0 + (\alpha + \gamma)/2\omega_0 \quad \text{S2.1}$$

Next we consider the interaction terms in details. Figure 1 shows that each TASR of the metamaterial can be represented as two kinds of electric dipole, and one kind of magnetic dipole. We therefore compute the interaction term of the Lagrangian by considering the dipole-dipole interactions between the resonators of the metamaterial.

The current density of a static electric dipole is  $\rho = -\nabla \cdot \mathbf{p}\delta^{(3)}$  (1995 J. Phys. A: Math. Gen. 28 4565), with this the interaction between two electric dipoles becomes (static approximation):

$$\int_{inter-TASR} d^3r(\rho\phi) = \mathbf{p}_1 \cdot \mathbf{E}_2 = \frac{3(\hat{\mathbf{r}}\cdot\mathbf{p}_1)(\hat{\mathbf{r}}\cdot\mathbf{p}_2) - \mathbf{p}_1\cdot\mathbf{p}_2}{4\pi\epsilon_0 r^3} \quad \text{S2.2}$$

where  $\mathbf{p}_1$  and  $\mathbf{p}_2$  are the two electrical dipole moments and  $\hat{\mathbf{r}}$  is the vector connecting them. Without loss of generality we can assume that  $\mathbf{p} = \mathbf{a}^{(p)}X$  (where  $\mathbf{a}^{(p)}$  is the polarizability constant), then:

$$\alpha = \alpha_0 \sum_{unit\ cells\ i,j} \frac{3(\hat{\mathbf{r}}_{ij}\cdot\mathbf{a}^{(p)}_i)(\hat{\mathbf{r}}_{ij}\cdot\mathbf{a}^{(p)}_j) - (\mathbf{a}^{(p)}_i\cdot\mathbf{a}^{(p)}_j)}{4\pi\epsilon_0 r_{ij}^3} \quad \text{S2.3}$$

Similarly for magnetic dipole the current density is  $\mathbf{J} = \nabla \times c\mathbf{m}\delta^{(3)}$

$$-\int d^3r \mathbf{A} \cdot \mathbf{J} = -c\mathbf{m}_1 \cdot \mathbf{B}_2 = \frac{3(\hat{\mathbf{r}} \cdot \mathbf{m}_1)(\hat{\mathbf{r}} \cdot \mathbf{m}_2) - \mathbf{m}_1 \cdot \mathbf{m}_2}{4\pi\epsilon_0 r^3} \quad \text{S2.4}$$

Magnetic dipoles are related to current density, the rate of change of charge density, whereas electric dipoles are related to charge density, it follows  $\mathbf{m} = \mathbf{a}^{(m)}\dot{X}/\omega_0$ , and

$$\gamma = \gamma_0 \sum_{\text{unit cells } i,j} \frac{3(\hat{\mathbf{r}}_{ij} \cdot \mathbf{a}^{(m)}_i)(\hat{\mathbf{r}}_{ij} \cdot \mathbf{a}^{(m)}_j) - \mathbf{a}^{(m)}_i \cdot \mathbf{a}^{(m)}_j}{4\pi\epsilon_0 r_{ij}^3} \quad \text{S2.5}$$

The above analysis only considered the dipole-dipole interactions between the TASRs. Yet the actual excitations induced in TASR by the incident light can be significantly more complex, requiring more multipole terms. Due to sub-wavelength size of the TASRs such extended multipole treatment is only necessary when considering the field scattered by TASRs at distance comparable to TASR size. In practice, this implies that high-order multipole treatment is only necessary for nearest-neighbor interactions. To account for this we introduce an extra frequency shift  $\Omega_{near}$ . The full expression for the resonant frequency of the metamaterial thus becomes:

$$\ddot{X} = -\Omega^2 X, \quad \Omega = \sqrt{\frac{\omega_0^2 + \alpha}{1 - \frac{\gamma}{\omega_0^2}}} \approx \omega_0 + \frac{(\alpha + \gamma)}{2\omega_0} + \Omega_{near} \quad \text{S2.6}$$

### Supplementary Note 3: Phase of electric and toroidal dipole

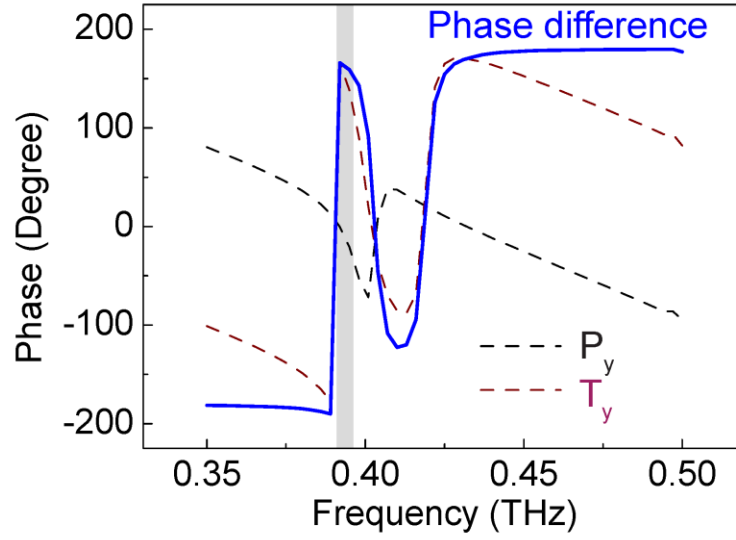


**Figure S1.** The retrieved phase information of electric and toroidal dipole for scenario S<sub>4</sub>. We see the opposite phase of electric and toroidal dipoles.

**Supplementary Note 4: Sample fabrication and measurements**

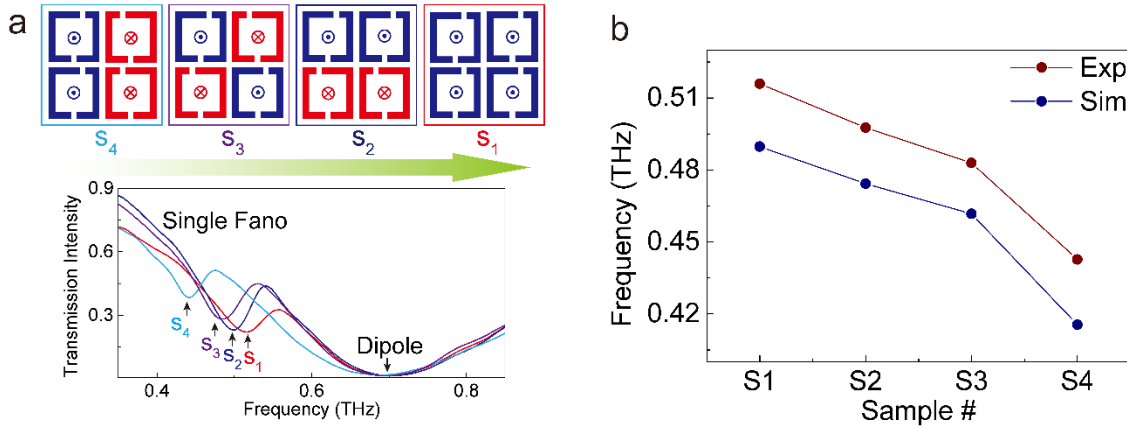


**Figure S2.** Measured Fano resonance frequencies of S<sub>1</sub> to S<sub>4</sub>. (a) Measured transmission spectra of S<sub>1</sub> to S<sub>4</sub>. The comparison of Fano resonance frequency of S<sub>1</sub> to S<sub>4</sub> obtained from experimental and simulated spectra.

The five samples were fabricated using the conventional flow of photolithography and thermal metallization. In the photolithography process, we performed the spin coating of photoresist, exposure under UV light with the predesigned mask and the development to get the complimentary photoresist pattern on the wafer. The samples would be finalized by the step of metallization and lifting off of the remaining photoresist through dissolving in acetone.

A fiber laser based terahertz time-domain spectroscopy system was used to measure the transmission spectra of the metamaterial samples and the reference (intrinsic silicon) in dry nitrogen atmosphere. The time-domain waveform was obtained on the basis of the time-resolved amplified voltage which is proportional to the amplitude of terahertz pulse. Fourier transform was performed to obtain the frequency domain spectra with both amplitude and phase information. The transmission amplitude spectra  $|\mathcal{T}(\omega)|$  and phase spectra  $\varphi(\omega)$  are calculated by  $\mathcal{T}(\omega) = \mathcal{T}^{\text{sam}}(\omega) / \mathcal{T}^{\text{ref}}(\omega)$  where  $\mathcal{T}^{\text{sam}}(\omega)$  is the complex transmission signal of samples and  $\mathcal{T}^{\text{ref}}(\omega)$  is the signal of reference, respectively. As shown in Figure S2a, we can clearly resolve the Fano resonance shift using the experimental setup, and the frequency shift exactly follows the simulated trend as shown in Figure S2b. An overall blueshift of experimental frequencies relative to simulations is due to difference in material parameters and other capacitive and inductive effects in experiments that were ignored in simulations.

### **Supplementary Note 5: Dipole-dipole interactions in S<sub>2</sub> and S<sub>4</sub>**

Here we illustrate that TASR-to-TASR dipole interactions in the case of S<sub>2</sub> and S<sub>4</sub>

metamaterials (Figures 2b and 2d respectively) suggest that resonant frequency of  $S_4$  metamaterial should be higher than that of  $S_2$ .

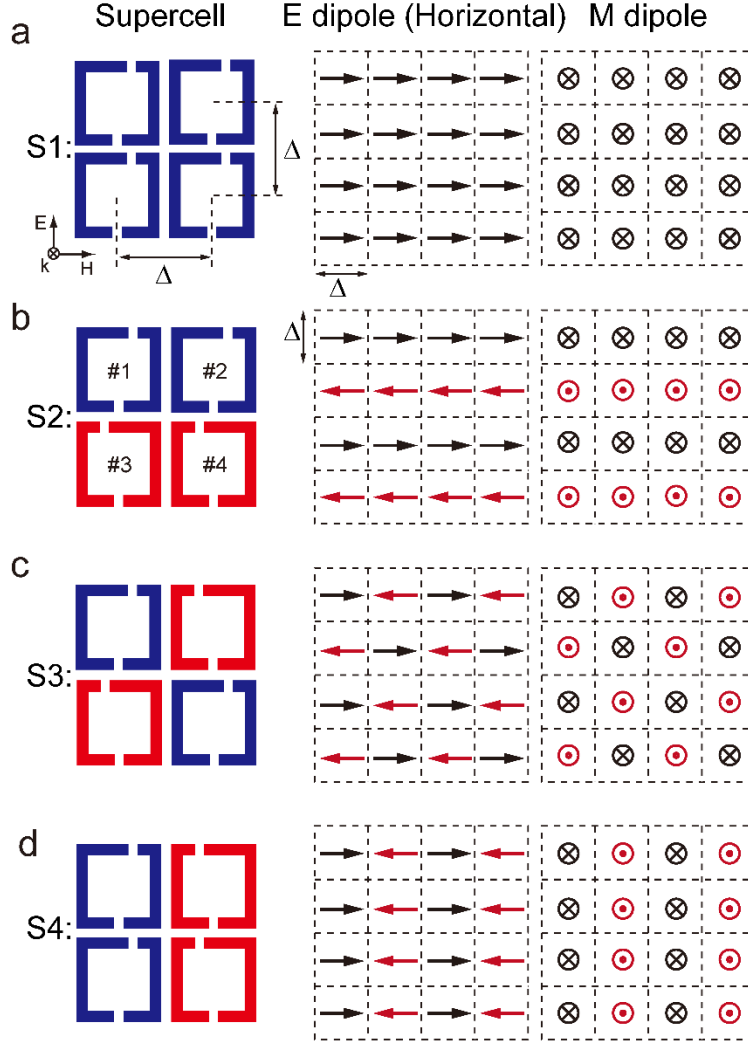


**Figure S3. Multipole analysis of metamaterials with supercells ( $S_1$ - $S_4$ ) consisting of four TASRs.** The configurations of the horizontal electric dipoles ( $P_x$ ) and out-of-plane magnetic dipole ( $M_z$ ) for the case of four supercells with four unit cells ( $S_1$ - $S_4$ ) at Fano resonance. The first column shows supercells consisting of quad-TASR, whereas the dipole plots in columns 2 and 3 show  $2 \times 2$  supercells, which translate to  $4 \times 4$  TASRs, in order to highlight emerging patterns. We denote the distance between the TASRs as  $\Delta$  in our calculations.

As discussed in the main paper, at trapped mode resonance, the response of a single TASR can be approximated by a vertical and horizontal electric dipole as well as out-of-plane

magnetic dipole (see Figure 1). The vertical electric dipole in all cases couples to incident radiation, and thus its orientation will be the same in all TASR (since the metamaterial is excited by uniform plane wave at normal incidence). What matters, therefore is the orientation of horizontal electric and out-of-plane magnetic dipoles, shown in Figure S3. In case of metamaterials  $S_2$  and  $S_4$ , the relative orientation of magnetic dipoles is the same up to 90-degree rotation, thus the only difference (for dipole-dipole interactions) is in the horizontal electric dipoles.

The  $S_2$  metamaterial corresponds head-to-tail orientation of horizontal electric dipoles within each row (low interaction energy), whilst  $S_4$  has head-to-head and tail-to-tail orientation within rows (high energy). Within each column  $S_2$  has alternating orientation of electric dipoles (low energy), whilst  $S_4$  has uniform orientation of electric dipoles in each column (high energy). Therefore, the dipole-dipole interaction energy in  $S_4$  should be higher than in  $S_2$  suggesting that its resonant energy should be higher (i.e. high  $\alpha$  implies high  $\Omega$  in Equation 2, given the same  $\omega_0$  and  $\gamma$ ), but in experiments we observe the opposite effect, suggesting that the response of TASR metamaterials is dominated by nearest-neighbor interactions ( $\Omega_{near}$  overrides  $\alpha$ ).

### **Supplementary Note 6: Optimization of asymmetry**



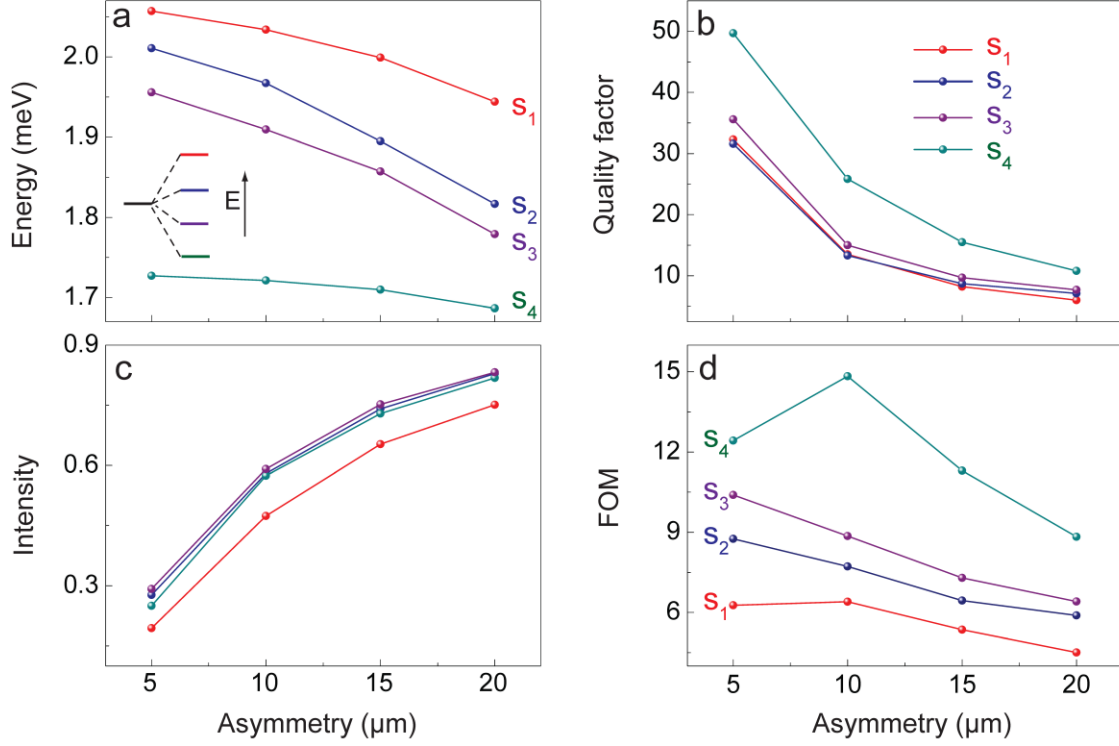


**Figure S4.** Resonance performance of individual Fano resonances in S<sub>1</sub>, S<sub>2</sub>, S<sub>3</sub>, and S<sub>4</sub> with different degree of asymmetry. (a) The evolution of resonance energy shifting. The Fano resonance evolution of (b) quality factor and (c) magnitude. (d) The FOM evolution of the individual Fano resonance.

The asymmetric TASR also provides another degree of freedom to tailor the scattering strength by changing the resonator asymmetry degree characterized by the parameter  $d$ . The lower asymmetry (smaller  $d$ ) would give rise to a weaker scattering by the electric dipole and thus a sharper resonance with lower resonant intensity (characterized by the peak to dip intensity of the resonance). We have investigated the performance of the Fano resonances with the supercells by varying  $d$  from 5 μm to 20 μm. As shown in Figure S4a, we could observe the evolution of the individual resonance energy levels for different supercell arrangements S<sub>1</sub>, S<sub>2</sub>, S<sub>3</sub> and S<sub>4</sub>. The overall resonance energy decreases with a

larger asymmetry degree which is ascribed to the weakened scattered power originating from the decreased power of magnetic dipole (spin) by the individual resonator. The other features to characterize the resonance properties are the quality factor and resonance intensity. As shown in Figure S4b, the destructive interference between electric and toroidal dipole in S<sub>4</sub> clearly enhance the  $Q$  factor by suppressing the radiative losses. The resonance intensity is also important for applications in order to record the spectral signature, and it is the scattered power of electric dipole that dominates the intensity of the Fano resonance. Therefore, the larger asymmetry would give rise to the stronger resonance intensity due to the stronger electric dipole as shown in Figure S4c. However, some real applications would require both high quality factor and large resonance intensity, and thus we estimate the tradeoff between these two parameters. We introduce the parameter, Figure of Merit (FOM), to describe the tradeoff that is defined as  $FOM = Q \times \Delta I$ , where  $Q$  is the value of quality factor and  $\Delta I$  is the Fano resonance intensity. As shown in Figure S4d, S<sub>4</sub> provides the best performance due to the destructive interference between toroidal and electric dipole enabling a much improved  $Q$  factor.

### **Supplementary Note 7: Experiment limitations**

1. We ignored the dispersion of metal and applying a DC value ( $3.56 \times 10^7$  S/m) for aluminum in simulations. This would not be a problem when the radiative loss of the resonator array is relatively large, for example in S<sub>1</sub> to S<sub>3</sub>, where we could observe the similar values of Fano quality factors between simulations and experiments. In the reference (Adv. Opt. Mater. 4 (3), 457-463, 2016), it was experimentally demonstrated that a DC value of metal excellently reproduces the real experimental scenario in terahertz

regime. However, when it comes to an extreme scenario in S<sub>4</sub> where the radiative loss is largely suppressed, the weak Ohmic loss from the metal plays a crucial role in determining the Fano lineshape. In order to keep consistency, we used the same DC conductivity and simulation approach to simulate all the samples, and this would lead to the difference between simulation and experiment for S<sub>4</sub>.

2. We assumed an infinite resonator array by applying the periodic boundary condition in simulations, however, in real experiments, finite resonators (~1,5000 resonators) were probed by the terahertz beam with a beam spot of 3.5 mm diameter in the beam waist. Although less radiation loss would be expected with more coherent resonators excited (Phys. Rev. Lett. 104, 223901 (2010)) due to the coherent resonance nature of Fano resonance, the number of excited resonators was enough for the quality factor to be saturated with weak radiation loss. However, fabrication defects were inevitable which would largely increase the radiation loss, thus resulting in a relative low quality factor in experiments.

3. The loss of materials in the metamaterial system also affects the spectral quality. Although intrinsic material losses were considered in simulations to better reproduce the exact experimental scenario, inevitable scattering losses (conductivity) due to rough surface of metal resonators and substrates (loss tangent) will largely affect the spectral quality, especially for high quality factor resonance mode (Adv. Opt. Mater. 4 (3), 457 (2016)). Although we used the high-resistivity silicon (>5,000 Ohm-cm) as substrate and aluminum ( $\sigma = 3.56 \times 10^7$  S/m) to fabricate the resonators in order to ensure low material losses in experiments, the scattering loss due to surface roughness reduces quality factor of

the measured spectra, resulting low resolution of the modes of  $S_1$  to  $S_3$  in the spectrum of  $S_5$ .

### Supplementary Note 8: Equivalence to Ising model

Here we will use the formalism of Hamiltonian mechanics to establish an analogy between the TASR metamaterial driven at Fano resonance, and the Ising model. The interaction part of the Hamiltonian for the Ising model is (D. V. Shroeder, “Thermal Physics” 2000, by Addison Wesley Longman):

$$H_{Is} = -\sum_{i=1}^N B\mu s_i - J \sum_{*i,j}^N s_i s_j \quad \text{S8.1}$$

where sums run over  $N$  particles. Above  $B$  is the applied magnetic field,  $s_i = \pm 1/2$  is projection of the spin along the  $z$ -axis,  $\mu$  is the magnetic dipole moment of a particle, and  $J$  is the coupling parameter that encodes the energy between neighboring particles. The ‘\*’ in the second sum denotes that it sums interactions of the nearest neighbors only.

Next, we consider the TASR metamaterial at Fano resonance. Each TASR is represented by a single dynamic variable  $x_i$  and is associated with a simple harmonic oscillator with resonant frequency ( $\omega_0$ ). The metamaterial is placed into an electromagnetic cavity, which supports even- and odd-parity electromagnetic plane-waves, described by the vector potential variables  $A_e$  and  $A_o$  respectively. Here we assume that electromagnetic waves of only one frequency ( $\omega$ ), and one polarization ( $\hat{\mathbf{x}}$ ) are involved, and that waves propagate along the  $z$ -axis. The electric ( $E$ ) and magnetic ( $B$ ) fields are then given by:

$$\mathbf{E}_{cav} = \hat{\mathbf{x}}(-\dot{A}_e \sin kz + \dot{A}_o \cos kz) \quad \text{S8.2}$$

$$\mathbf{B}_{cav} = \hat{\mathbf{y}}k(A_e \cos kz + A_o \sin kz) \quad \text{S8.3}$$

With some standard manipulations one can show that the Hamiltonian for the metamaterial cavity system must be:

$$H_{MM} = \sum_i \frac{p_i^2 + \omega_0^2 x_i^2}{2} - \sum_i ax_i \dot{A}_0 - \sum_{i<j} (\alpha_{ij} x_i x_j + \beta_{ij} x_i p_j + \zeta_{ij} p_i p_j) \quad \text{S8.4}$$

$$+ \sigma \left( \frac{1}{2} (P_e^2 + \omega^2 A_e^2 + P_o^2 + \omega^2 A_o^2) + A_o F_o + A_e F_e \right)$$

where  $P_{e,o}$  are conjugate momenta of  $A_{e,o}$ . Constants  $\alpha_{ij}, \beta_{ij}, \zeta_{ij}$  describe interactions of TASR loops with each other. Constants  $\sigma$  is related to the size of the considered cavity. The effect of the incident THz-waves is accounted for by the external driver terms:  $F_e$  and  $F_o$ .

Clearly, the second and third terms of the Hamiltonian above map directly into the standard Ising model. The incident radiation now takes the role of the applied magnetic field in the original Ising model. The change in temperature in the case of TASR metamaterial corresponds to change of geometry, whilst the microstates correspond to the different collective modes supported by the metamaterial under plane-wave excitation. For any specific geometry, under plane-wave illumination, the TASR metamaterial can support several collective excitations (corresponds to microstates) with certain amplitude (corresponds to probability amplitude).

### Order parameter

Order parameter is often a starting point for the analysis of a thermodynamic system. It is commonly a number that is zero in one phase of the system and becomes nonzero as the phase of the system changes. In Ising model, the order parameter is the magnetization per

spin of the system (C. Kittel, “Thermal Physics”, 1980, W. H. Freeman; Second edition edition). Here we shall suggest a suitable order parameter analogue for the TASR metamaterial.

In principle, by analogy with Ising model, the order parameter for TASR metamaterial should be related to the excitations of individual TASRs, however such excitations can only be observed in near-field measurements (due to sub-wavelength size of the metamaterial lattice). A more suitable parameter for far-field observations is the coherence area of the reflected light (J. W. Goodman “Statistical Optics” 2000 JOHN WILEY & SONS, INC). Coherence area can be thought of the area of the source, here TASR metamaterial (in reflection), that radiates as a plane-wave source. If all the TASRs of the metamaterial oscillate in phase, the coherence area of the emitted light will include all of metamaterial. If all the TASRs in the metamaterial oscillate randomly, coherence area will be minimized. Since, the coherence area of the light reflected by the metamaterial will depend on the coherence area of the input light, we propose the following order parameter:

$$\eta = (\mathcal{A}_r - \mathcal{A}_i)/p^2 \tag{S8.5}$$

where  $\mathcal{A}_r$  is the coherence area of the reflected light,  $\mathcal{A}_i$  is the coherence area of the incident light and  $p^2$  is the metamaterial unit cell area. Clearly the order parameter has to be measured with spatially incoherent incident light, and will depend chiefly on the geometry of the sample rather than the properties of incident radiation. We note in passing that a somewhat similar experiment has already been conducted on TASR-like metamaterials which display cooperative resonant response. In (V. A Fedotov, J. Wallauer, M. Walther, M. Perino, N. Papasimakis and N. I. Zheludev, “Wavevector Selective Metasurfaces and Tunnel Vision Filters”, Light: Sci. App. 4, e306 (2015)) such

metamaterial was used to rectify the wavefront of the incident radiation, by filtering out components of the incident light which did not correspond to normally incident plane wave radiation.

### **Entropy**

Due to linearity of Maxwell's equations, and due to discrete nature of the metamaterial (i.e. each unit cell is finite in size), the equations of motion of the TASR metamaterial can always be recast into the form of a matrix equation:

$$\begin{pmatrix} \ddot{x}_1 \\ \ddot{x}_2 \\ \vdots \end{pmatrix} = \mathbf{M} \cdot \begin{pmatrix} x_1 \\ x_2 \\ \vdots \end{pmatrix} + \mathbf{b} \quad \text{S8.6}$$

where matrix  $\mathbf{M}$  contains information on dynamics of the system (resonant frequencies, strength of coupling between individual TASRs etc), whilst vector  $\mathbf{b}$ , would contain the boundary conditions and the external driver. We will assume that harmonic solution does exist and that, therefore vector  $\mathbf{b}$  lies in the space spanned by the  $N_b$  orthonormal eigenvectors of  $\mathbf{M}$  ( $N_b \leq N$ ; where  $N$  is the number of unit cells in the metamaterial). The number of accessible modes in the metamaterial will therefore be  $N_b$ . One can use this to get entropy of the excitation in the TASR metamaterial:

$$S = -k_b \sum_{q=1}^{N_b} p_q \log p_q \quad \text{S8.7}$$

where  $k_b$  is the Boltzmann constant. The sum above runs over the accessible orthonormal eigenstates of matrix  $\mathbf{M}$ . The 'probability' of each eigenstate corresponds to the ratio of the energy in the given eigenstate compared to full energy stored at the metamaterial.

### **Thermodynamic energy**

Another quantity necessary for the thermodynamic analogy is thermodynamic energy stored in the system ( $U$ ). The actual electromagnetic energy captured by the metamaterial is not suitable since it would depend on the intensity of the incident radiation, whilst other quantities we have defined thus far do not.

In defining the entropy we have assumed that the response of the metamaterial will be decomposable into  $N_b$  orthogonal eigenmodes, which will operate as harmonic oscillators. It is relatively simple to prove that given two simple harmonic oscillators described by Hamiltonians:

$$H_{i=1,2} = \frac{p_i^2}{2} + \omega_i^2 \frac{x_i^2}{2} \quad \text{S8.8}$$

The time-averaged energy stored in them, i.e. the time-average of the Hamiltonian, will be  $\langle H_i \rangle = \omega_i^2 \langle x_i^2 \rangle$ . Thus assuming that the amplitude of oscillations of the two harmonic oscillators is equal, the oscillator storing more energy would be the one with higher resonant frequency, and the scaling is  $\langle H_i \rangle \propto \omega_i^2$ . We therefore propose to define the thermodynamic energy as:

$$U \propto \Omega^2 \quad \text{S8.9}$$

where  $\Omega$  is the frequency of the Fano resonance. This approach agrees with the results in the Supplementary Note 2, where the strength of coupling between different TASRs, i.e. the magnitude of the interaction energy, has been shown to affect the resonant frequency of the Fano resonance.

### **Temperature**

The temperature of our analogue of the Ising model can then be defined through the entropy and energy. Conventionally, the temperature is related to these two quantities through (C.



Kittel, “Thermal Physics”, 1980, W. H. Freeman; Second edition edition):

$$\frac{1}{T} = \left( \frac{\partial S}{\partial U} \right)_{\text{other free relevant parameter}} \quad \text{S8.10}$$

In case of TASR metamaterial, it follows that the “temperature” should be:

$$\theta_{TASR} = \kappa / \left( \frac{\partial S}{\partial \Omega^2} \right) = -k_b \kappa / \left( \frac{\partial \sum_{q=1}^{N_b} p_q \log p_q}{\partial \Omega^2} \right) \quad \text{S8.11}$$

where  $\kappa$  is a constant with suitable units,  $S$  is entropy and  $\Omega$  is the resonant frequency of the Fano mode. Since  $\theta_{TASR}$  is related to changes in resonant frequency of the metamaterial, it must be related to the physical configuration of the TASR metamaterial, i.e. change in “temperature” can only be achieved through change in geometry or change in ambient refractive index. Unlike with order parameter the quantities required for  $T_{TASR}$  should be measured under plane-wave illumination in order to effectively engage the Fano mode.

### **Supplementary Note 9: Quantitative comparison of interactions in TASR supercell metamaterials**

Arguments relying on interaction energy have played a large role in our discussion in this work. Here we shall provide a simple way of quantifying the interaction energy. In line with standard notions, we take the full time-averaged energy of the time-harmonic electromagnetic system as (assuming unit relative permeability):

$$U = \frac{1}{2} \Re \left( \int d^3r (E^* \cdot D + H^* \cdot B) \right) = \frac{1}{2} \Re \left( \int d^3r (\epsilon_0 \epsilon_r |E|^2 + \mu_0^{-1} |H|^2) \right) \quad \text{S9.1}$$

The interaction energy of the metamaterial is the part of the energy that depends on the distance between the unit cells. By simulating the response of the metamaterials and integrating (numerically) the expression in Eq. S9.1, and using the polynomial series in

unit cell size (period of a single resonator,  $p$ ), one can get the series:

$$U - \langle U \rangle_p = \frac{1}{p}U_1 + \frac{1}{p^2}U_2 + \frac{1}{p^3}U_3 + \frac{1}{p^4}U_4 + \dots \quad \text{S9.2}$$

where  $\langle U \rangle_p$  is the average of the interaction energy for the considered unit cell sizes. The electromagnetic field due to dipoles, both electric and magnetic, decays as 1<sup>st</sup> -3<sup>rd</sup> power with the interaction distance. One can therefore define the dipole-dipole interaction energy as:

$$U_{dipole} = \frac{1}{p}U_1 + \frac{1}{p^2}U_2 + \frac{1}{p^3}U_3 \quad \text{S9.3}$$

and the nearest-neighbor interaction energy as the remaining part:

$$U_{nn} = U - \langle U \rangle_p - U_{dipole} \quad \text{S9.4}$$

That is, the nearest-neighbor interaction energy will be the ‘error’ in fitting ( $U - \langle U \rangle_p$ ) with

power series  $\frac{1}{p}U_1 + \frac{1}{p^2}U_2 + \frac{1}{p^3}U_3$ .

Having introduced the theory, we now move to numerical results. In order to estimate the range of interaction energy, we performed the simulations of S4 by changing the unit cell size  $p$  from 75  $\mu\text{m}$  to 85  $\mu\text{m}$  with step size of 1  $\mu\text{m}$ . The full energy (S9.1) for metamaterials with different unit cell sizes is shown in Figure S5.

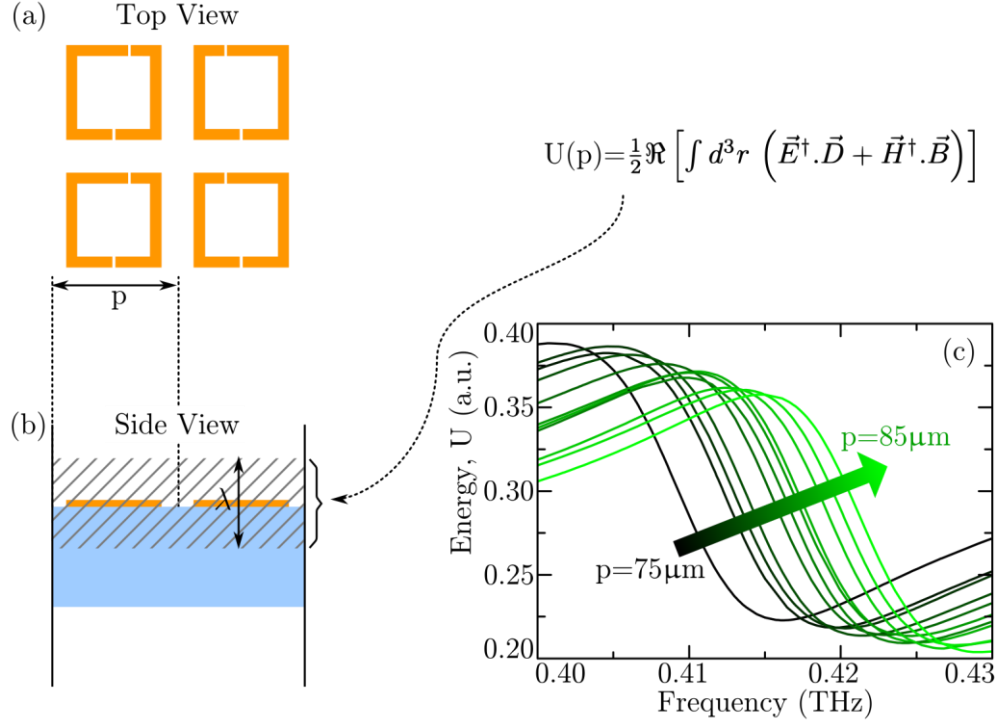


**Figure S5.** The procedure for finding the energy  $U$ . (a)-(b) show the combined unit cell of the TASR. The energy is obtained by integrating Eq. S9.1 over the volume, shown by the shaded area in (b). The volume fills the whole unit cell and stretches for a full free-space wavelength along the third dimension. (c) Shows the simulation results of the energy obtained for different periods ( $p$ ), for the TASR metamaterials.

The dipole and nearest-neighbor interaction energy was obtained in the following fashion. First, the time-averaged energy in the metamaterial, as a function of the reciprocal metamaterial period  $p$  from  $75 \mu\text{m}$  to  $85 \mu\text{m}$  with step size of  $1 \mu\text{m}$ , was numerically simulated as shown in Figure S5c. Cubic fit to the simulated energy with different lattice periods was performed to obtain  $U_1$ ,  $U_2$ , and  $U_3$  using Eq. S9.3. These coefficients were then used to obtain the dipole interaction energy ( $U_{\text{dipole}}$ ) for the representative

metamaterial period of  $p=80 \mu\text{m}$ . Finally, the dipole and the nearest-neighbor interaction energy was computed using the chosen period and the polynomial fitting coefficients, according to Eq. S9.3 and S9.4. The nearest-neighbor interaction energy acts as the ‘error’ in fitting  $(U - \langle U \rangle_p)$  with power series  $\frac{1}{p}U_1 + \frac{1}{p^2}U_2 + \frac{1}{p^3}U_3$ . The interaction energy for the dipole and nearest-neighbor is shown in Figure S6. As one can see, the nearest-neighbor interactions turn out to be of the same order as the dipole interactions.

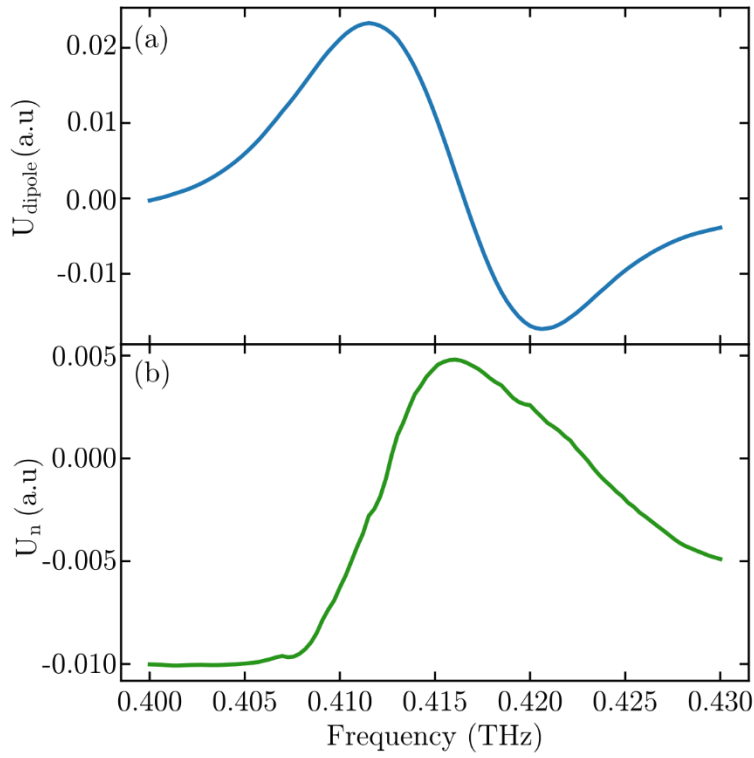


**Figure S6.** The interaction energy for dipole (a) and nearest-neighbor (b) interactions as defined in Eq. S9.3 and Eq. S9.4 for single resonator spacing at  $p=80 \mu\text{m}$ .